

# PI3K $\gamma$ Mediates Kaposi's Sarcoma-Associated Herpesvirus vGPCR-Induced Sarcomagenesis

Daniel Martin,<sup>1</sup> Rebeca Galisteo,<sup>1</sup> Alfredo A. Molinolo,<sup>1</sup> Reinhard Wetzker,<sup>2</sup> Emilio Hirsch,<sup>3</sup> and J. Silvio Gutkind<sup>1,\*</sup>

<sup>1</sup>Oral and Pharyngeal Cancer Branch, National Institute of Dental and Craniofacial Research, National Institutes of Health, Bethesda, MD 20892, USA

<sup>2</sup>Institute of Molecular Cell Biology, Center for Molecular Biomedicine, Jena University Hospital, University Jena, Jena 07745, Germany

<sup>3</sup>Department of Genetics, Biology and Biochemistry, Biotechnology Center, School of Medicine, University of Torino, Torino 10126, Italy

\*Correspondence: [sg39v@nih.gov](mailto:sg39v@nih.gov)

DOI 10.1016/j.ccr.2011.05.005

## SUMMARY

Angioproliferative tumors induced by the Kaposi's sarcoma-associated herpesvirus (KSHV) have been successfully treated with rapamycin, which provided direct evidence of the clinical activity of mTOR inhibitors in human malignancies. However, prolonged mTOR inhibition may raise concerns in immunocompromised patients, including AIDS-Kaposi's sarcoma (KS). Here, we explored whether KSHV oncogenes deploy cell type-specific signaling pathways activating mTOR, which could be exploited to halt KS development while minimizing immune suppressive effects. We found that PI3K $\gamma$ , a PI3K isoform exhibiting restricted tissue distribution, is strictly required for signaling from the KSHV-encoded vGPCR oncogene to Akt/mTOR. Indeed, by using an endothelial-specific gene delivery system modeling KS development, we provide genetic and pharmacological evidence that PI3K $\gamma$  may represent a suitable molecular target for therapeutic intervention in KS.

## INTRODUCTION

The activation of the PI3K/Akt/mTOR-signaling axis may represent one of the most frequent events in cancer (Bunney and Katan, 2010; Manning and Cantley, 2007; Sabatini, 2006), hence prompting the development of molecular inhibitors of this biochemical route as promising anticancer agents, many of which are already in advanced stages of clinical evaluation (Bunney and Katan, 2010; Dancey, 2010; Guertin and Sabatini, 2007). In this regard the effectiveness of an mTOR inhibitor, rapamycin, as an antitumoral agent was first demonstrated for the treatment of an angioproliferative disease known as Kaposi's sarcoma (KS) arising in immunosuppressed renal transplanted patients (Stallone et al., 2005). Rapamycin and its analogs (rapalogs) are currently under intense investigation for their clinical efficacy in numerous cancer types (Dancey, 2010). Four clinical manifestations of KS differ in their aggressiveness and epidemiology (Ganem, 2010). The mildest form, classic KS, affects elder men of

the Mediterranean area. Endemic KS is much more aggressive and is now the leading cancer affecting children and young men in subequatorial Africa. Iatrogenic and AIDS-associated KS are the most aggressive, and related to immunosuppression due to organ transplantation or HIV infection, respectively (Ganem, 2010; Mesri et al., 2010).

The Kaposi sarcoma-associated herpesvirus (KSHV), also known as human herpesvirus 8 (HHV-8), is the etiologic agent of KS (Chang et al., 1994; Ganem, 2010; Mesri et al., 2010). KSHV encodes 84 genes and 12 miRNAs, many of which harbor oncogenic potential (Ganem, 2010). Among them, several lines of evidence support the role for a constitutively active, virally encoded G protein-coupled receptor (vGPCR) in KS initiation and progression (Bais et al., 2003; Mesri et al., 2010; Montaner et al., 2003; Yang et al., 2000). vGPCR activates an intricate network of molecular-signaling events, driving both the aberrant growth of endothelial cells and the paracrine transformation of endothelial-derived cells expressing KSHV latent genes (Mesri

## Significance

Activation of the PI3K-Akt pathway resulting in mTOR stimulation is one of the most frequent events in human cancer; hence, small molecule inhibitors of this biochemical route represent attractive anticancer agents. However, key immune and metabolic functions of mTOR may limit the clinical benefits of its specific inhibitors for cancer treatment. The activation of a tissue-restricted PI3K isoform, PI3K $\gamma$ , by the KSHV-encoded vGPCR oncogene enabled inhibition of an upstream event contributing to oncogenic signaling to mTOR, while sparing the normal physiological functions of mTOR. These findings indicate that PI3K $\gamma$  may represent a suitable therapeutic target for KS and for a myriad of angioproliferative diseases, including tumor-induced angiogenesis, thereby avoiding the potential toxicities associated with mTOR, Akt, or pan PI3K inhibition.

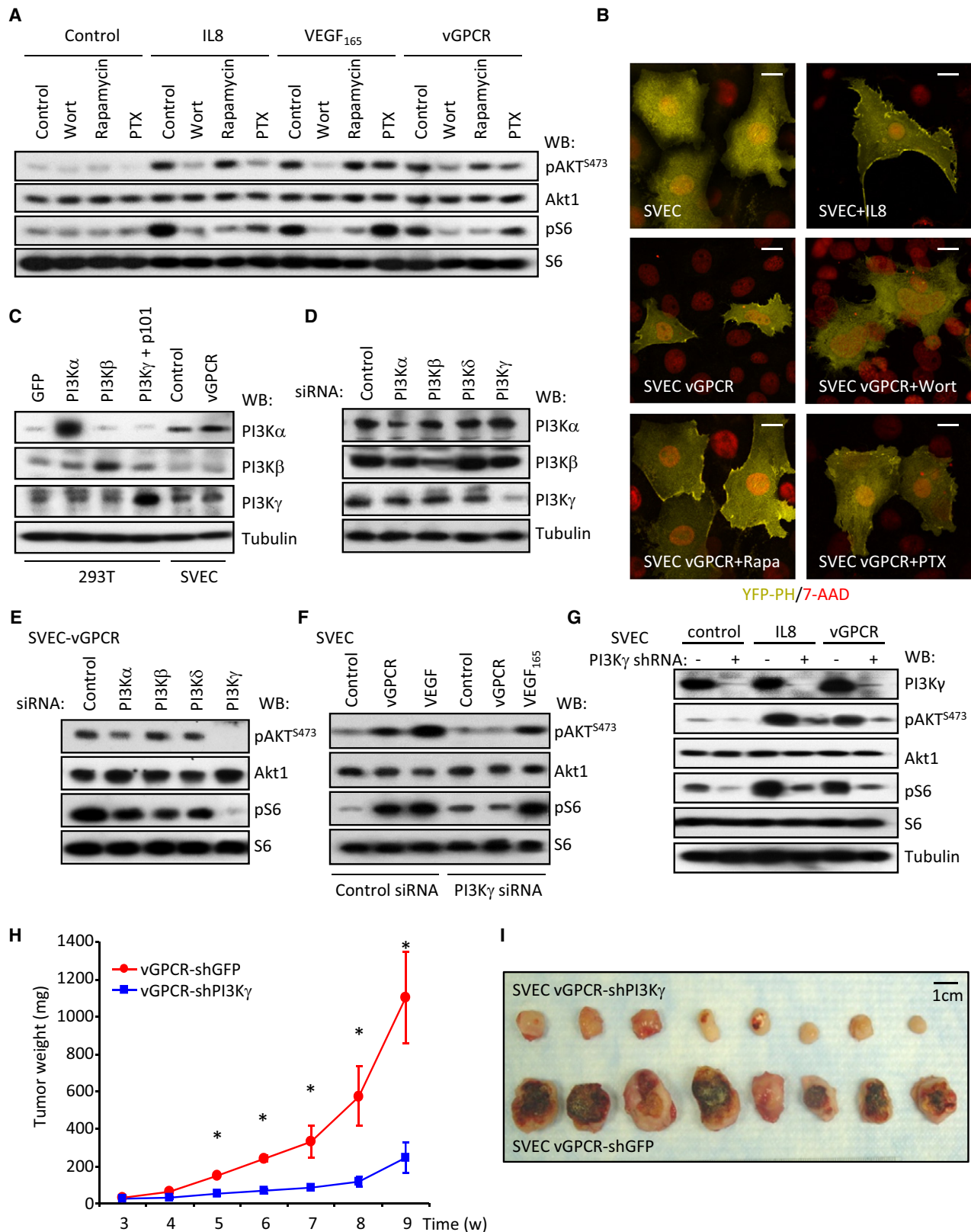


**Figure 1. vGPCR Induces the PI3K $\gamma$ -Dependent Activation of mTOR**

(A) Serum-starved murine immortal endothelial cells (SVECs) were pretreated with inhibitors and then stimulated with IL8 or VEGF<sub>165</sub> (see Supplemental Experimental Procedures for details). vGPCR, SVECs stably expressing vGPCR.

et al., 2010). The PI3K/Akt/mTOR pathway represents one of the most prominent oncogenic mechanisms deployed by vGPCR, as revealed by genetically defined animal models for KS (Sodhi et al., 2004, 2006). These findings provided the foundation for the evaluation and clinical success of the use of mTOR inhibitors for iatrogenic KS lesions, achieving a rapid and complete remission in all the patients involved in the initial study (Stallone et al., 2005). The effectiveness of rapamycin in iatrogenic KS may result from a rare convergence of antitumoral and desirable therapeutic immunosuppressive properties; hence, rapamycin is now becoming the standard of care for renal transplanted patients developing KS (Stallone et al., 2008). However, prolonged use of mTOR inhibitors may raise concerns for those affected by the endemic form of this disease and for patients with AIDS that are already immunocompromised due to their elevated viral load. In this regard, the possibility still exists that KSHV oncogenes may deploy cell type-specific signaling events leading to mTOR activation that can be exploited to halt KS development while minimizing immune suppressive effects. Thus, we set up to investigate the molecular mechanism by which vGPCR initiates the oncogenic activation of mTOR in endothelial cells, aimed at identifying alternative molecular targets for the treatment of angioproliferative diseases.

## RESULTS

Expression of vGPCR in immortalized murine (SVECs) and human (HMEC-1) endothelial cells stimulates Akt and mTOR potently, as judged by the accumulation of phosphorylated Akt (pAkt<sup>S473</sup>) and S6 (pS6), the latter a downstream target of mTOR (Figure 1A; see Figure S1A available online). This was accompanied by morphological changes (Figure S1B), increased cell size (Figure S1C), and increased survival upon growth factor deprivation (Figure S1D). Activation of Akt and mTOR required PI3K because it is sensitive to the PI3K inhibitor wortmannin, whereas pS6 accumulation was blocked by rapamycin that inhibits mTOR. Inhibition of heterotrimeric G proteins of the G $_i$  family by pertussis toxin (PTX) partially prevented the activation of Akt and mTOR by vGPCR. The CXC chemokine IL8, which acts on endogenous G $_i$ -coupled CXCR2 receptors, and VEGF, which stimulates its cognate tyrosine kinase receptors, were used as positive and negative controls, respectively.

These results were further confirmed using the pleckstrin homology (PH) domain from Akt fused to YFP, which can be used to monitor the presence of phosphatidylinositol 3,4,5-trisphosphate (PIP $_3$ ) at the plasma membrane. IL8 treatment or the expression of vGPCR induced the relocalization of the PH-YFP construct from the cytosol to the plasma membrane (Figure 1B; Figure S1E), which was sensitive to wortmannin and PTX, but not to rapamycin. The residual activity after PTX treatment may reflect the more limited ability of vGPCR to signal to Akt by other PTX-insensitive G proteins. We can conclude that a G $_i$ -dependent PI3K activity is largely required for the activation of the Akt/mTOR pathway by vGPCR.

Four different class I PI3K catalytic subunits have been described in mammalian cells, which display divergent regulation and patterns of expression. PI3K $\alpha$ ,  $\beta$ , and  $\delta$  are regulated by tyrosine kinase receptors through interaction with their regulatory subunits, with PI3K $\alpha$  and  $\beta$  being expressed ubiquitously and PI3K $\delta$  expressed mainly by leukocytes (Engelman et al., 2006). PI3K $\gamma$  exhibits restricted tissue distribution and is activated by GPCRs by the interaction of its catalytic (p110 $\gamma$ ) and regulatory subunit (p101) with G $_{\beta\gamma}$  subunits (Lopez-Illasaca et al., 1997). PI3K $\alpha$ ,  $\beta$ , and  $\gamma$  isoforms were readily detectable in endothelial cells (Figure 1C; Figure S1A), as reported (Morello et al., 2009), whereas PI3K $\delta$  was undetectable by western blotting and qPCR (data not shown). PI3K $\gamma$  knockdown with specific siRNAs resulted in a dramatic decrease in the activation of Akt/mTOR in endothelial cells expressing vGPCR (Figures 1D and 1E), whereas knockdown of PI3K $\alpha$  or PI3K $\beta$  had only a limited effect. In contrast, PI3K $\gamma$  siRNA did not interfere with the ability to stimulate Akt/mTOR upon VEGF $_{165}$  treatment (Figure 1F). Because PI3K $\gamma$  is expressed in human KS lesions (Figure S1F), we hypothesized that PI3K $\gamma$  may represent an attractive candidate to transduce the signal initiated by vGPCR to Akt/mTOR in endothelial-derived tumor cells. Based on these findings, we analyzed the impact of PI3K $\gamma$  on vGPCR-induced tumorigenesis in endothelial xenograft models (Montaner et al., 2003). We first identified PI3K $\gamma$  short hairpin RNAs (shRNAs) whose stable expression efficiently knocks down the expression of PI3K $\gamma$  (Figure 1G), and reduced the activation of Akt and mTOR in response to either IL8 treatment or vGPCR cotransfection. Remarkably, knockdown of PI3K $\gamma$  greatly impaired the ability of vGPCR to form tumors in nude mice when compared to shRNA-expressing

(B) SVEC vGPCR cells expressing YFP-PH (see Supplemental Experimental Procedures) were treated as indicated. See quantification in Figure S1. Scale bars equal 20  $\mu$ m.

(C) Analysis of the expression of the PI3K  $\alpha$ ,  $\beta$ , and  $\gamma$  isoforms in SVECs. Expression of the different PI3K isoforms was analyzed by western blotting. Over-expressing 293T cells were used as controls.

(D) siRNA-mediated knockdown of different PI3K isoforms in SVECs. SVECs were transfected with siRNAs as depicted (Supplemental Experimental Procedures). Exponentially growing cultures were analyzed by western blot after 5 days.

(E) PI3K $\gamma$  mediates the activation of Akt and mTOR downstream of vGPCR. SVEC vGPCR cells transfected as in (D) were analyzed by western blotting as indicated after 5 days.

(F) PI3K $\gamma$  knockdown selectively impairs the activation of Akt and mTOR downstream of vGPCR, but not VEGF $_{165}$ . SVEC (Control, VEGF) and SVEC vGPCR (vGPCR) cells were treated as depicted and analyzed by western blotting.

(G) shRNA-mediated knockdown of PI3K $\gamma$  reduces the activation of Akt and mTOR induced by IL8 and vGPCR expression. SVEC and SVEC vGPCR cells transfected with PI3K $\gamma$  shRNA expression vectors for 72 hr were treated as described in Experimental Procedures. A western blot analysis of a representative experiment is shown.

(H) SVEC vGPCR cells stably expressing a PI3K $\gamma$  shRNA show reduced tumorigenesis in nude mice. One million SVEC vGPCR PI3K $\gamma$  or GFP shRNA cells (see Supplemental Experimental Procedures) were injected subcutaneously into the flanks of nude mice and allowed to form tumors. Graph represents the mean tumor weight ( $n = 8$ )  $\pm$  SEM (\* $p \leq 0.001$ ) at each time point.

(I) Gross morphology of the tumor xenografts from (H).

See also Figure S1.

control cells (Figures 1H and 1I). Together, these results suggest that PI3K $\gamma$  may play an essential role in vGPCR-induced activation of Akt/mTOR and in vGPCR-initiated sarcomagenesis.

We next sought to challenge these observations in a genetically defined *in vivo* KS model. In particular we have previously generated genetically engineered animals expressing the receptor for the avian leukosis virus (ALV) *Tva* under the control of the *Tie2* endothelial-specific promoter (Figure 2A) (Montaner et al., 2003). In this system, infection of *Tie2-Tva* mice with ALV-derived RCAS retroviruses encoding vGPCR or the potent oncogene polyoma middle T antigen (PyMT) induces the *Tva*-dependent death of mice within only a few weeks (Montaner et al., 2003). We backcrossed this animal line into a PI3K $\gamma$  knockout background (Hirsch et al., 2000) generating mice bearing none ( $^{+/+}$ ), hemizygous ( $^{-/+}$ ), and homozygous ( $^{-/-}$ ) deletion of this gene. Of note, PI3K $\gamma$  knockout mice are viable and display only reduced inflammatory responses and impaired neutrophil and monocyte migration *in vivo* (Ruckle et al., 2006). Infection with RCAS PyMT resulted in the deaths of approximately 60% of the TVA-positive mice within 50 days postinfection, regardless of their genotype for PI3K $\gamma$  (Figure 2B), in agreement with the mechanism of action of this viral oncogene, involving PI3K $\alpha$  and PI3K $\beta$  (Dilworth, 2002). However, when RCAS vGPCR retroviruses were injected, 77.7% of the TVA(+)/PI3K $^{+/+}$  mice died within 70 days (median survival 20 days;  $n = 9$ ), but only 20% of the TVA(+)/PI3K $^{-/+}$  died after 150 days ( $n = 10$ ;  $p = 0.0024$ ; with respect to PI3K $^{+/+}$  mice), whereas all of the TVA(+)/PI3K $^{-/-}$  mice survived ( $n = 7$ ;  $p = 0.0004$ ; with respect to PI3K $^{+/+}$  mice) without showing signs of disease, even after 9 months of observation. The cause of death was attributed to the presence of multiple internal angioproliferative lesions. Those TVA(+)/PI3K $^{+/+}$  animals that did not die within the initial 70 day period (22.3%) invariably started developing external and internal KS-like lesions after 6 months, in agreement with previous reports (Montaner et al., 2003), but no PI3K $^{-/+}$  and PI3K $^{-/-}$  mice developed lesions even after prolonged observation (Figure 2C).

These findings provided a strong rationale for exploring whether pharmacological inhibition of PI3K $\gamma$  represents a therapeutic strategy to treat KS. As a proof of principle, we assessed whether AS-605240, a widely used PI3K $\gamma$  inhibitor, can prevent vGPCR-induced sarcomagenesis. AS-605240 induced a remarkable and dose-dependent inhibition of Akt and mTOR activation in endothelial cells expressing vGPCR (Figure 3A; Figure S2A). We further examined the function of this PI3K $\gamma$  inhibitor by analyzing the subcellular localization of GFP-FoxO1, which is excluded from the nucleus upon phosphorylation by Akt (Brunet et al., 2004). As shown in Figures 3B and 3C, AS-605240 inhibited Akt downstream of vGPCR, as depicted by the nuclear localization of GFP-FoxO1, using as a control a nuclear-localized FoxO1 mutant (GFP-FoxO1 AAA) that is resistant to Akt-mediated inactivation. Treatment with rapamycin led to only a subtle decrease in Akt activity (Figure 3D), probably reflecting a delayed inhibition of the mTOR complex 2 by rapamycin (Laplanche and Sabatini, 2009). Furthermore, treatment of vGPCR-expressing cells with AS-605240 resulted in a dose-dependent inhibition of proliferation and decreased viability (Figure S2B). In addition to promoting the direct transformation of endothelial cells, vGPCR expression can promote the tumoral growth of endothe-

lial cells, including those expressing latent KSHV transcripts in a paracrine fashion (Mesri et al., 2010; Montaner et al., 2003). This observation prompted us to explore the potential role of PI3K $\gamma$  in vGPCR-initiated paracrine signaling. For this analysis we took advantage of prior observations that vGPCR-expressing cells promote the proliferation and activation of NF $\kappa$ B of endothelial cells in a paracrine fashion. As shown in Figures S2C and S2D, inhibition of PI3K $\gamma$  in vGPCR-expressing endothelial cells by the use of specific shRNAs or by the use of PI3K $\gamma$  inhibitors nearly abolished the ability of vGPCR-expressing cells to release pro-proliferative (Figures S2C and S2D) and NF $\kappa$ B-activating (Figure S2E) soluble factors.

To test the potential therapeutic properties of PI3K $\gamma$  inhibition, nude mice bearing endothelial-vGPCR tumors were treated with AS-605240, showing a marked reduction in tumor growth (Figure 4A) with minimal signs of toxicity ( $2.11\% \pm 0.9\%$  body weight loss after 5 days). The impact of PI3K $\gamma$  inhibition was found to be highly specific under these conditions (Figure 4B) because AS-605240 did not inhibit Akt<sup>S473</sup> or S6 phosphorylation caused by PyMT expression (Figure 4C) or affect the growth of SVEC-PyMT tumor xenografts (Figure 4D). Inhibition of the mTOR pathway as judged by pS6 immunostaining was complete 24 hr after the initiation of the treatment (Figure 4E), to an extent similar to that seen with rapamycin. We also generated endothelial cells expressing vGPCR and the red fluorescent mCherry protein, which allowed visualizing the tumor growth in real time. Treatment with both rapamycin and AS-605240 greatly reduced both the size and fluorescence of the tumors to the same extent (Figures 4F and 4G). Further analysis of tumor biopsies revealed that both treatments induced a marked reduction of cell proliferation as measured by Ki-67 staining and increased the number of apoptotic cells, as determined by active caspase 3 (Figure 4H). Taken together, these results indicate that PI3K $\gamma$  inhibition with AS-605240 is at least as effective as rapamycin at reducing the activity of mTOR, resulting in reduced cell proliferation and the apoptotic demise of cancer cells and the consequent tumor regression.

Collectively, *in vitro* and *in vivo* experiments using endothelial cells, tumor xenografts, and endothelial-specific gene delivery systems in genetically defined animals support the key role of the vGPCR-PI3K $\gamma$  signaling axis in KS initiation and progression, hence representing a candidate molecular target for pharmacological intervention in KS.

## DISCUSSION

The dissection of the dysregulated signaling networks leading to tumor initiation and malignant progression has recently afforded the opportunity of developing molecular-targeted options for cancer prevention and treatment. Recent studies have highlighted the central role of the PI3K/Akt/mTOR pathway in some of the most prevalent human neoplasias (Bunney and Katan, 2010). In this regard, each PI3K isoform may perform distinct functions (Engelman et al., 2006; Vanhaesebroeck et al., 2005), thus suggesting that their selective inhibition may provide therapeutic opportunities in specific disease conditions while limiting their side effects. For example, PI3K $\delta$ , which is expressed in few immune-derived cells, is now being evaluated as a specific target for multiple hematologic malignancies (Ameriks and



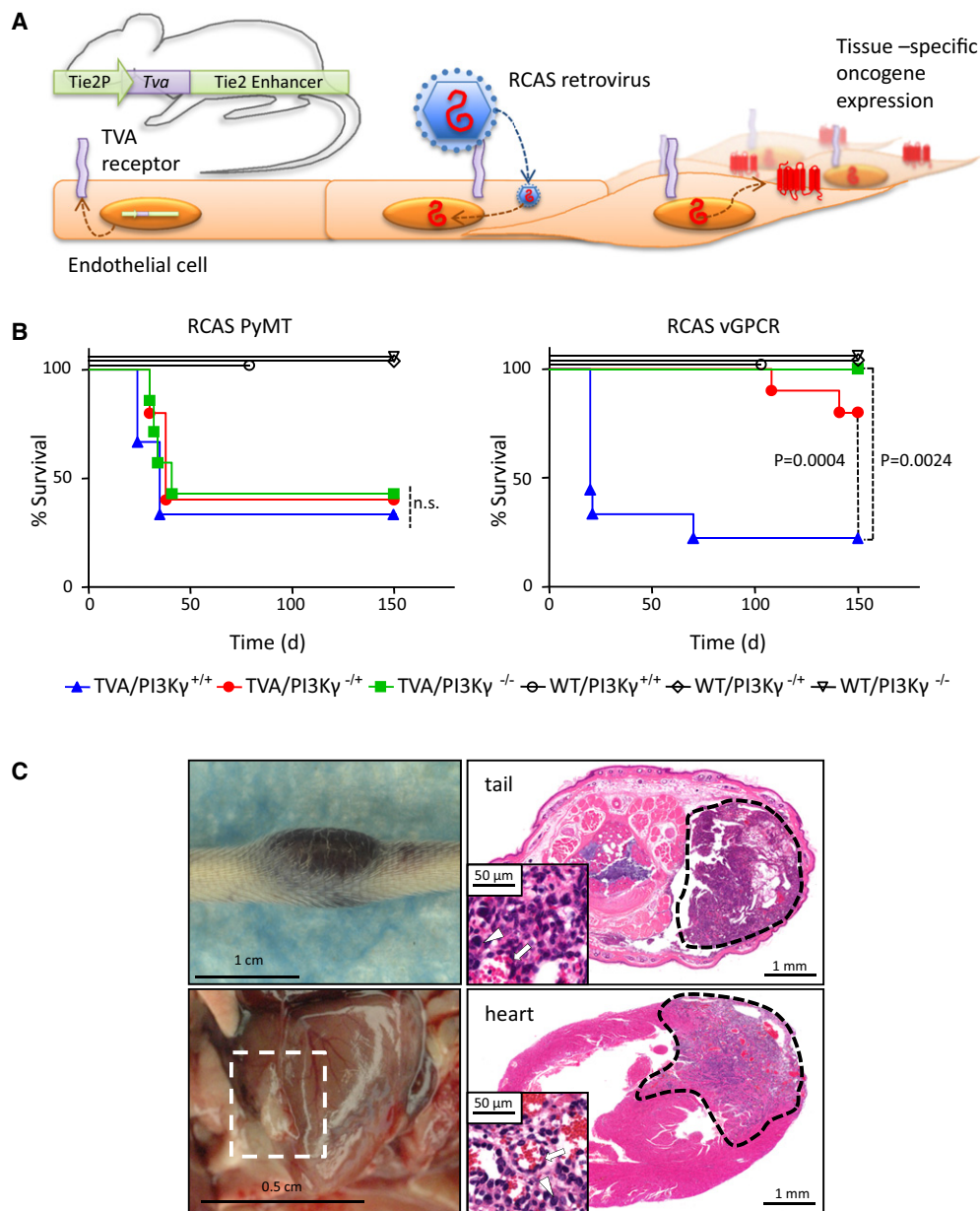


**Figure 2. A Genetic Model Unveils the Requirement of PI3K $\gamma$  for vGPCR-Induced Sarcomagenesis**

(A) Schematic overview of the RCAS system for somatic gene transfer. Tissue-restricted expression of the ALV receptor TVA is achieved by transgenic technology. The *Tie2* promoter and enhancer sequences target the expression of TVA to endothelial tissues. RCAS viruses encoding a gene of interest are injected into mice resulting in tissue-specific targeted infection and expression of the viral payload.

(B) Effect of the hemi- and homozygotic loss of expression of PI3K $\gamma$  on animal survival after infection with RCAS virus on TIE2-TVA animals. Five-day-old mice born from TIE2-TVA/PI3K $\gamma^{+/+}$   $\times$  PI3K $\gamma^{-/-}$  breeding pairs were injected with RCAS-PyMT virus ( $5.0 \times 10^7$  infective units) (right panel), or RCAS vGPCR ( $5.0 \times 10^7$  infective units) (left panel). Animals' deaths occurred naturally and were recorded and correlated to the presence of multiple internal angioproliferative lesions during the necropsy. The dashed box depicts a representative macroscopic lesion in the heart. The dashed lines outline typical KS-like lesions in the tail and heart, as indicated, which are shown under higher magnification in the corresponding insets. Arrowheads show spindle cells, and arrows indicate atypical vessels.

(C) Left-upper and lower panels show gross appearance of representative KS lesions appearing in TIE2-TVA mice injected with RCAS vGPCR that survived longer than 150 days. Right panels demonstrate H&E section of the lesions found in the tail and heart. Insets illustrate high-power magnification of the same field. Several other tissues, including lung and kidneys, displayed similar lesions.

Venable, 2009). Here, we provide genetic evidence that PI3K $\gamma$ , a PI3K isoform exhibiting a restricted tissue distribution and regulated by a distinct mechanism from other Class I PI3Ks (Morello et al., 2009), is strictly required for the growth of endo-

thelial-derived tumors and the development of KS-like lesions. Furthermore, we show that PI3K $\gamma$ -specific inhibitors promote the rapid decrease in Akt and mTOR activation caused by expression of a KSHV oncogene, vGPCR, in endothelial cells,

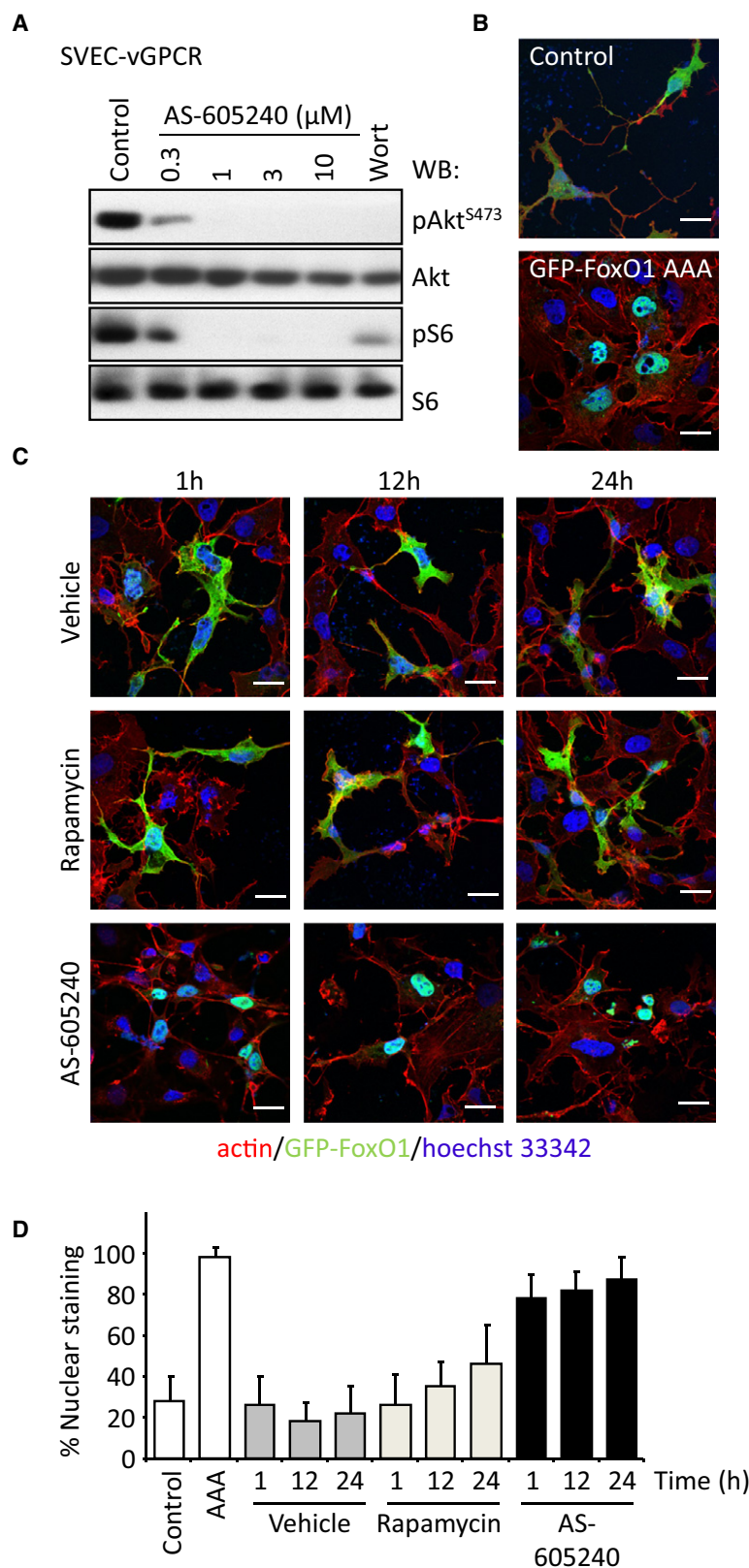


**Figure 3. Pharmacological Inhibition of PI3K $\gamma$  Reduces the Activity of the Akt/mTOR Pathway by vGPCR In Vitro**

(A) Serum-starved SVEC-vGPCR cells were treated with increasing concentrations of AS-605240, a PI3K $\gamma$ -specific inhibitor, or wortmannin (Wort) for 1 hr. Protein lysates were analyzed by western blotting. A representative blot is shown.

(B) A GFP-FoxO1 construct was used as reporter for Akt activity. COS-7 cells were cotransfected with a vGPCR-encoding plasmid and GFP-FoxO1 (Control) or a GFP-FoxO1 in which the three residues phosphorylated by Akt responsible for its nuclear export are mutated to alanine (GFP-FoxO1 AAA). Serum-starved cells were fixed and stained with phalloidin-Texas red and the nuclear staining Hoechst 33342. In the upper panel, control cells display typical GFP cytosolic localization. In the lower panel, cells expressing the AAA mutant show a strong nuclear localization of this construct. Scale bars, 25  $\mu$ m.

(C) Inactivation of Akt induced by treatment with AS-605240. COS-7 cells expressing vGPCR and GFP-FoxO1, as in (B), were treated as indicated. AS-605240 induced a strong and sustained inhibition of Akt, as reflected by the nuclear relocalization of GFP-FoxO1, whereas rapamycin only inhibited Akt modestly after 24 hr. Scale bars, 25  $\mu$ m.

(D) Quantification of the percentage of cells displaying nuclear translocation of the GFP-FoxO1 constructs from (B) and (C). Bars represent the mean percentage  $\pm$  SD from 3 different samples in which at least 200 transfected cells were evaluated. See also Figure S2.

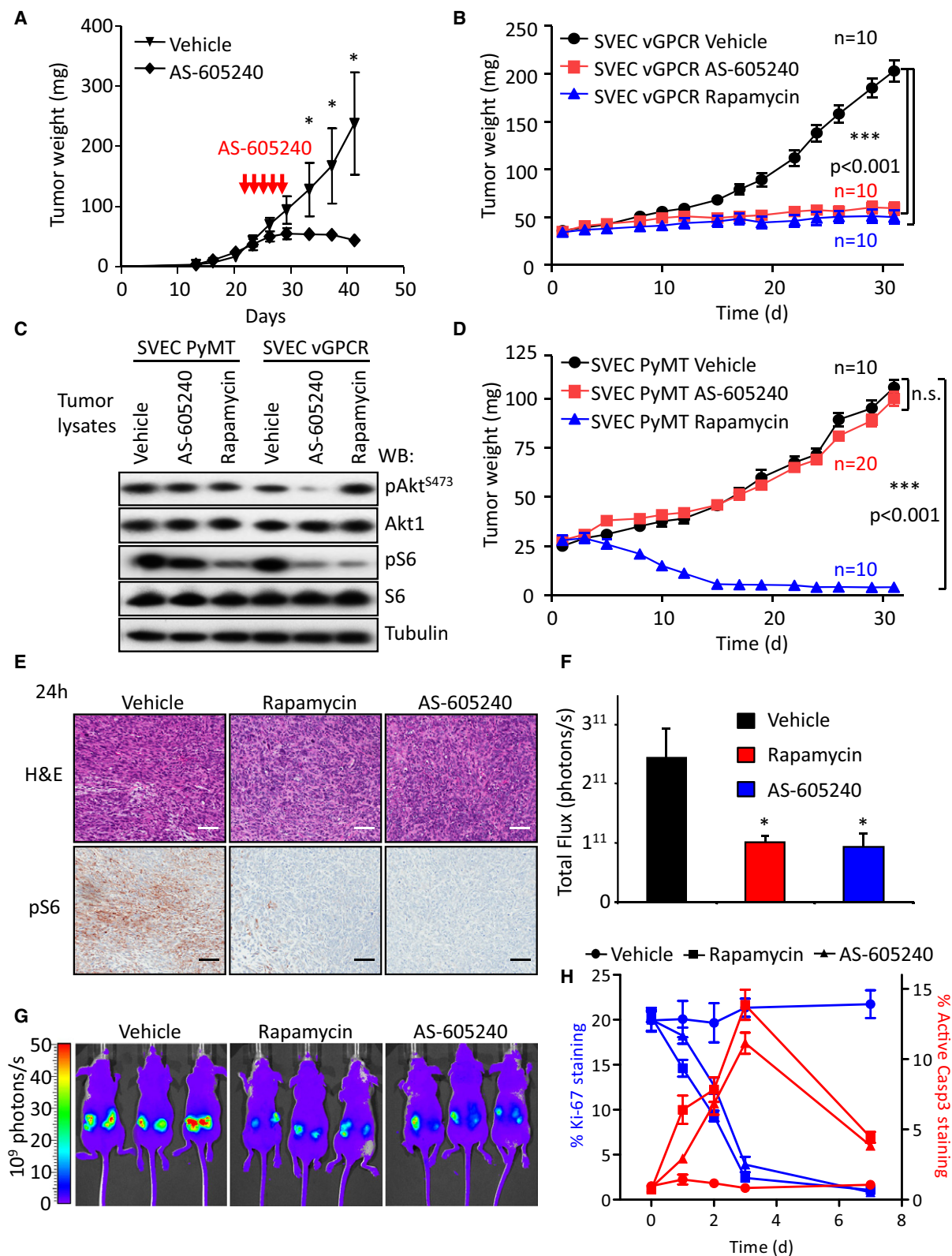


**Figure 4. PI3K $\gamma$  Inhibition Halts Tumor Growth Induced by vGPCR**

(A) SVEC vGPCR xenografts were prepared as in Figure 1H. Tumors were allowed to grow for 3 weeks (average tumor weight  $42.3 \pm 2.3$  mg), and mice were treated with vehicle or 25 mg/kg AS-605240 twice daily i.p. for 5 consecutive days. Animal weight was monitored for signs of toxicity. Data points represent mean tumor weight  $\pm$  SEM (n = 8). \*p < 0.001.

thereby causing their apoptotic death and tumor regression, probably due to impaired vGPCR-initiated direct and paracrine-transforming mechanisms.

Extensive studies in mice lacking PI3K $\gamma$  have demonstrated that this protein is not required for normal development, life span, or basic immune responses, unless under stress conditions, and suggest that PI3K $\gamma$  may represent a suitable therapeutic target in a variety of inflammatory and cardiovascular diseases (Ghigo et al., 2010; Ruckle et al., 2006). Interestingly, even the deletion of a single PI3K $\gamma$  allele in heterozygous mice was sufficient to prevent the formation of KS-like lesions and protected the majority of the mice from KSHV vGPCR-caused death, highlighting the exquisite sensitivity of endothelial-derived tumors to PI3K $\gamma$  inhibition. Taken together, these findings raise the possibility that PI3K $\gamma$  inhibitors may represent a suitable therapeutic option to prevent or treat already-established KS lesions, likely avoiding the potential toxicities associated with mTOR, Akt, or pan-PI3K inhibition.

KS remains the most prevalent cancer among children and adolescents in Africa, and whereas the use of highly active anti-retroviral therapy (HAART) has dramatically reduced the number of AIDS-KS cases in the last decade, KS is still the most prevalent AIDS-associated malignancy (Ganem, 2010). Failure to adhere to the HAART regime, aging, chronic inflammation, and the possibility of the emergence of HAART-resistant HIV all pose a risk of KS reemergence that we cannot afford to ignore. In this regard, maintaining a normal immunocompetence appears to be the most effective way to control KS. Paradoxically, the efficacy of the immunosuppressant rapamycin at treating iatrogenic KS highlights the sensitivity to targeted molecular intervention in this angioproliferative disease despite a depressed immune status (Stallone et al., 2008). This, in turn, may facilitate the development of effective mechanism-based therapies for KS in patients in whom the risk for complications derived from immunosuppression outweighs the advantages of direct mTOR inhibition. Indeed, we now show that the distinct coupling ability of a KSHV oncogene to an endothelial-expressed PI3K isoform and the strict requirement of a functional PI3K $\gamma$  for KS development can be exploited for the development of molecular-targeted treatment options and preventive strategies for this viral-associated malignancy. The emerging role of PI3K $\gamma$  in pathological endothelial cell functions and malignant

conversion suggests that this PI3K isoform may also represent an attractive candidate for other angioproliferative diseases.

## EXPERIMENTAL PROCEDURES

### Cell Lines, Tissue Culture, DNAs, Transfections, and Reagents

SV40-immortalized murine endothelial cells (SVEC4-10) were purchased from ATCC (Manassas, VA, USA). SVEC and COS-7 cells were cultured in DMEM 10% fetal bovine serum supplemented with antibiotics, 5% CO<sub>2</sub> at 37°C. SVEC vGPCR cells were generated by stable transfection of pCEFL AU5-vGPCR as reported (Montaner et al., 2003). For stable knockdown, SVEC vGPCR cells were stably transfected with both shRNAs by cotransfection at 1:10 ratio with a Hygromycin-resistant vector (pBABE-hygro) and then selected in 150  $\mu$ g/ml Hygromycin for 2 weeks.

### Animal Work

All animal studies were carried out according to NIH-approved protocols, in compliance with the *Guide for the Care and Use of Laboratory Animals*.

### Establishment of Tumor Xenografts in Athymic nu/nu Mice

SVEC lines were used to induce endothelial tumor xenografts in athymic mice as described previously (Montaner et al., 2003).

TIE2-Tva transgenic animals (Montaner et al., 2003) were backcrossed into a PI3K $\gamma$  knockout background to generate the six possible combinations of Tva and PI3K $\gamma$  gene dosage. Preparation and in vivo infection with RCAS viruses encoding PyMT and AU5-tagged vGPCR were performed as previously described (Montaner et al., 2003).

### In Vivo Fluorescence Analysis

SVEC vGPCR cells were infected with a lentivirus encoding an EF-1 $\alpha$ -driven red fluorescent protein (pLESIP mCherry) and selected by FACS. Xenografts arising from these cells were quantified with a Xenogen IVIS-100 system (Caliper, Hopkinton, MA, USA) using the built-in Ds-Red filter set and 1 s exposure time. Measurements were performed using Caliper's Living Image suite.

### Statistical Analysis

Data analysis was performed using GraphPad Prism version 5.01 for Windows (GraphPad Software, San Diego, CA, USA). ANOVA followed by the Tukey t test was used to analyze the differences between experimental groups. Comparison of survival curves was performed by a log rank Mantel-Cox test.

## SUPPLEMENTAL INFORMATION

Supplemental Information includes Supplemental Experimental Procedures and two figures and can be found with this article online at doi:10.1016/j.ccr.2011.05.005.

(B) Tumor xenografts of SVEC vGPCR were established as described in Experimental Procedures. Tumors were treated with vehicle, AS-605240 (25 mg/kg/day i.p.), or rapamycin (5 mg/kg/day i.p.), as indicated. Tumor size was measured three times a week. Values represent mean tumor weight  $\pm$  SEM.

(C) Western blot analysis of pAkt<sup>S473</sup> and pS6 in SVEC PyMT or SVEC vGPCR tumor tissues collected 4 hr after i.p. injection of the indicated treatments, as described in (B) and (D).

(D) Tumor xenografts of SVEC PyMT were established and treated as in (B). Tumor size was measured three times a week. Values represent mean tumor weight  $\pm$  SEM. n.s., not significant.

(E) SVEC vGPCR tumor-bearing mice received one treatment with vehicle, rapamycin (5 mg/kg, i.p.), or AS-605240 (25 mg/kg, i.p.) and were sacrificed 24 hr after. Tumors were excised and processed for H&E and pS6 immunohistochemistry. A representative field is shown from four tumor samples with similar results. Bar, 150  $\mu$ m.

(F) Tumor xenografts were generated as in (A) using SVEC vGPCR cells expressing the red fluorescent protein mCherry. Tumor growth can be monitored in real time using in vivo fluorescence imaging. Tumors were allowed to grow for 3 weeks and then treated daily with vehicle, rapamycin (5 mg/kg), or AS-605240 (25 mg/kg), i.p. Photometric analysis of the tumors' red fluorescence after 1 month of treatment shows marked reduction in size in the rapamycin- and AS-605240-treated groups. Bars represent the average total flux ( $n = 10$  tumors)  $\pm$  SEM. \* $p \leq 0.01$ .

(G) Three representative animals of each group ( $n = 5$ ) from (F) are shown.

(H) Tumors generated in parallel as in (A) were excised and processed for immunostainings for the proliferation marker Ki-67 and the apoptotic marker cleaved Caspase3 (Active Casp3) after the indicated days of treatment. Representative areas of every preparation were automatically quantified by software analysis (Supplemental Experimental Procedures). Data points represent the mean percentage  $\pm$  SEM of positive cells in each preparation.



## ACKNOWLEDGMENTS

This research was supported by a National Institutes of Health Intramural AIDS Targeted Antiviral Program and the National Institute of Dental and Craniofacial Research. We thank M. Simaan and P. Amornphimoltham for their help and expert advice with the fluorescence microscopy studies. We apologize to colleagues whose primary research papers may not have been cited due to space constraints.

Received: October 2, 2010

Revised: March 5, 2011

Accepted: April 25, 2011

Published: June 13, 2011

## REFERENCES

- Ameriks, M.K., and Venable, J.D. (2009). Small molecule inhibitors of phosphoinositide 3-kinase (PI3K) delta and gamma. *Curr. Top. Med. Chem.* 9, 738–753.
- Bais, C., Van Geelen, A., Eroles, P., Mutlu, A., Chiozzini, C., Dias, S., Silverstein, R.L., Rafii, S., and Mesri, E.A. (2003). Kaposi's sarcoma associated herpesvirus G protein-coupled receptor immortalizes human endothelial cells by activation of the VEGF receptor-2/ KDR. *Cancer Cell* 3, 131–143.
- Brunet, A., Sweeney, L.B., Sturgill, J.F., Chua, K.F., Greer, P.L., Lin, Y., Tran, H., Ross, S.E., Mostoslavsky, R., Cohen, H.Y., et al. (2004). Stress-dependent regulation of FOXO transcription factors by the SIRT1 deacetylase. *Science* 303, 2011–2015.
- Bunney, T.D., and Katan, M. (2010). Phosphoinositide signalling in cancer: beyond PI3K and PTEN. *Nat. Rev. Cancer* 10, 342–352.
- Chang, Y., Cesarman, E., Pessin, M.S., Lee, F., Culpepper, J., Knowles, D.M., and Moore, P.S. (1994). Identification of herpesvirus-like DNA sequences in AIDS-associated Kaposi's sarcoma. *Science* 266, 1865–1869.
- Dancey, J. (2010). mTOR signaling and drug development in cancer. *Nat. Rev. Clin. Oncol.* 7, 209–219.
- Dilworth, S.M. (2002). Polyoma virus middle T antigen and its role in identifying cancer-related molecules. *Nat. Rev. Cancer* 2, 951–956.
- Engelman, J.A., Luo, J., and Cantley, L.C. (2006). The evolution of phosphatidylinositol 3-kinases as regulators of growth and metabolism. *Nat. Rev. Genet.* 7, 606–619.
- Ganem, D. (2010). KSHV and the pathogenesis of Kaposi sarcoma: listening to human biology and medicine. *J. Clin. Invest.* 120, 939–949.
- Ghigo, A., Damilano, F., Braccini, L., and Hirsch, E. (2010). PI3K inhibition in inflammation: toward tailored therapies for specific diseases. *Bioessays* 32, 185–196.
- Guertin, D.A., and Sabatini, D.M. (2007). Defining the role of mTOR in cancer. *Cancer Cell* 12, 9–22.
- Hirsch, E., Katanaev, V.L., Garlanda, C., Azzolino, O., Pirola, L., Silengo, L., Sozzani, S., Mantovani, A., Altruda, F., and Wymann, M.P. (2000). Central role for G protein-coupled phosphoinositide 3-kinase gamma in inflammation. *Science* 287, 1049–1053.
- Laplanche, M., and Sabatini, D.M. (2009). mTOR signaling at a glance. *J. Cell Sci.* 122, 3589–3594.
- Lopez-Illasaca, M., Crespo, P., Pellici, P.G., Gutkind, J.S., and Wetzker, R. (1997). Linkage of G protein-coupled receptors to the MAPK signaling pathway through PI 3-kinase gamma. *Science* 275, 394–397.
- Manning, B.D., and Cantley, L.C. (2007). AKT/PKB signaling: navigating downstream. *Cell* 129, 1261–1274.
- Mesri, E.A., Cesarman, E., and Boshoff, C. (2010). Kaposi's sarcoma and its associated herpesvirus. *Nat. Rev. Cancer* 10, 707–719.
- Montaner, S., Sodhi, A., Molinolo, A., Bugge, T.H., Sawai, E.T., He, Y., Li, Y., Ray, P.E., and Gutkind, J.S. (2003). Endothelial infection with KSHV genes in vivo reveals that vGPCR initiates Kaposi's sarcomagenesis and can promote the tumorigenic potential of viral latent genes. *Cancer Cell* 3, 23–36.
- Morello, F., Perino, A., and Hirsch, E. (2009). Phosphoinositide 3-kinase signaling in the vascular system. *Cardiovasc. Res.* 82, 261–271.
- Ruckle, T., Schwarz, M.K., and Rommel, C. (2006). PI3Kgamma inhibition: towards an 'aspirin of the 21st century'? *Nat. Rev. Drug Discov.* 5, 903–918.
- Sabatini, D.M. (2006). mTOR and cancer: insights into a complex relationship. *Nat. Rev. Cancer* 6, 729–734.
- Sodhi, A., Montaner, S., Patel, V., Gomez-Roman, J.J., Li, Y., Sausville, E.A., Sawai, E.T., and Gutkind, J.S. (2004). Akt plays a central role in sarcomagenesis induced by Kaposi's sarcoma herpesvirus-encoded G protein-coupled receptor. *Proc. Natl. Acad. Sci. USA* 101, 4821–4826.
- Sodhi, A., Chaisuparat, R., Hu, J., Ramsdell, A.K., Manning, B.D., Sausville, E.A., Sawai, E.T., Molinolo, A., Gutkind, J.S., and Montaner, S. (2006). The TSC2/mTOR pathway drives endothelial cell transformation induced by the Kaposi's sarcoma-associated herpesvirus G protein-coupled receptor. *Cancer Cell* 10, 133–143.
- Stallone, G., Schena, A., Infante, B., Di Paolo, S., Loverre, A., Maggio, G., Ranieri, E., Gesualdo, L., Schena, F.P., and Grandaliano, G. (2005). Sirolimus for Kaposi's sarcoma in renal-transplant recipients. *N. Engl. J. Med.* 352, 1317–1323.
- Stallone, G., Infante, B., Grandaliano, G., Schena, F.P., and Gesualdo, L. (2008). Kaposi's sarcoma and mTOR: a crossroad between viral infection neo-angiogenesis and immunosuppression. *Transpl. Int.* 21, 825–832.
- Vanhaesebroeck, B., Ali, K., Bilancio, A., Geering, B., and Foukas, L.C. (2005). Signalling by PI3K isoforms: insights from gene-targeted mice. *Trends Biochem. Sci.* 30, 194–204.
- Yang, T.Y., Chen, S.C., Leach, M.W., Manfra, D., Homey, B., Wiekowski, M., Sullivan, L., Jenh, C.H., Narula, S.K., Chensue, S.W., and Lira, S.A. (2000). Transgenic expression of the chemokine receptor encoded by human herpesvirus 8 induces an angioproliferative disease resembling Kaposi's sarcoma. *J. Exp. Med.* 191, 445–454.